

# 1 Quantifying camouflage and conspicuousness using visual salience

2 Thomas W. Pike\*

3 *School of Life Sciences, University of Lincoln, Lincoln, LN2 2UU*

4 \*Correspondence to: [tpike@lincoln.ac.uk](mailto:tpike@lincoln.ac.uk)

5

6 1. Being able to quantify the conspicuousness of animal and plant colouration is key to  
7 understanding its evolutionary and adaptive significance. Camouflaged animals, for  
8 example, are under strong selection pressure to minimise their conspicuousness to potential  
9 predators. However, successful camouflage is not an intrinsic characteristic of an animal,  
10 but rather an interaction between that animal's phenotype and the visual environment that  
11 it is viewed against. Moreover, the efficacy of any given camouflage strategy is determined  
12 not by the signaller's phenotype per se, but by the perceptual and cognitive capabilities of  
13 potential predators. Any attempts to quantify camouflage must therefore take both  
14 predator perception and the visual background into account.

15 2. Here I describe the use of species-relevant saliency maps, which combine the different  
16 visual features that contribute to selective attention (in this case the luminance, colour and  
17 orientation contrasts of features in the visual environment) into a single holistic measure of  
18 target conspicuousness. These can be tuned to the specific perceptual capabilities of the  
19 receiver, and used to derive a quantitative measure of target conspicuousness.  
20 Furthermore, I provide experimental evidence that these computed measures of  
21 conspicuousness significantly predict the performance of both captive and wild birds when  
22 searching for camouflaged artificial prey.

23 3. By allowing the quantification of prey conspicuousness, saliency maps provide a useful  
24 tool for understanding the evolution of animal signals. However, this is not limited to  
25 inconspicuous visual signals, and the same approach could be readily used for quantifying  
26 conspicuous visual signals in a wide variety of contexts, including, for example, signals  
27 involved in mate choice and warning colouration.

28 **Keywords:** Selective attention, signal evolution, crypsis, visual salience, conspicuousness

29

## 30 **Introduction**

31 Being able to attend to relevant objects in a cluttered visual scene has considerable  
32 evolutionary significance because it allows an animal to rapidly identify potential food,  
33 mates and predators. Indeed, some stimuli are intrinsically conspicuous, or salient, in a  
34 given context; for example, in humans a ripe red fruit among green leaves automatically and  
35 involuntarily attracts attention (Frey *et al.* 2011). Saliency is independent of the nature of  
36 the particular task, operates very rapidly, and is primarily driven in a bottom-up manner that  
37 reflexively directs visual focus based on certain low-level visual features (e.g. colour,  
38 orientation and/or brightness contrasts). If a stimulus is sufficiently salient, it will therefore  
39 'pop out' of a visual scene (Itti & Koch 2001). As a result, the concept of visual salience has  
40 clear implications for understanding the evolution of animal signals which, broadly speaking,  
41 either aim to maximise saliency (as in the case of animals producing conspicuous mating  
42 signals) or minimise it (as in animals that rely on camouflage to avoid detection by potential  
43 predators) (Ruxton, Sherratt & Speed 2004; Endler & Mielke 2005; Stevens & Merilaita  
44 2009).

45 However, despite its importance, predicting an animal's salience from its visual appearance  
46 remains a major challenge. This is in part because saliency is not an intrinsic characteristic of  
47 an animal, but rather an interaction between that animal's phenotype and the visual  
48 environment that it is viewed against which, in nature, is likely to be heterogeneous and  
49 visually cluttered (Godfrey, Lythgoe & Rumball 1987; Merilaita 2003; Dimitrova & Merilaita  
50 2014). Because of this, an animal that is well camouflaged against one background may be  
51 highly salient against another; any useful measure of saliency must therefore take into  
52 account the relative characteristics of both the target and its background (Xiao & Cuthill  
53 2016). Moreover, conspicuousness is determined not by the signaller's visual phenotype per  
54 se, but is a function of the perceptual and cognitive capabilities of potential receivers (They  
55 & Casas 2002; Stevens & Cuthill 2006; Osorio & Vorobyev 2008; Chiao *et al.* 2009). Different  
56 species vary in their perceptual abilities (e.g. in the spectral sensitivity of their retinal  
57 photoreceptors) and in the cognitive mechanisms underpinning how perceptual information  
58 is processed and integrated (Kesner & Olton 2014), and this will necessarily impact on how  
59 salient prey with particular phenotypic characteristics appear. Animals which appear highly  
60 salient to one receiver may completely lack salience for another, even against the same

61 visual background, emphasising the importance of incorporating species-relevant  
62 perceptual and cognitive information into estimates of salience wherever possible (Xiao &  
63 Cuthill 2016; Troscianko, Skelhorn & Stevens 2017).

64 To address the challenge of quantifying an animal's visual salience a wide variety of metrics  
65 have been suggested, some of which are inspired by known features of animals' visual and  
66 cognitive systems. These include metrics for quantifying internal and external edges  
67 (Stevens & Cuthill 2006; Lovell *et al.* 2013; Webster *et al.* 2013; Kang *et al.* 2015; Troscianko,  
68 Skelhorn & Stevens 2017), the orientation of which often contrasts with those in the  
69 background or with edges intrinsic to the prey itself; those involving pattern detection or  
70 the identification of pattern contrasts (Spottiswoode & Stevens 2010; Stoddard, Kilner &  
71 Town 2014; Troscianko *et al.* 2016; Troscianko, Skelhorn & Stevens 2017); those which  
72 calculate chromatic (Kang *et al.* 2015) or luminance (i.e. perceived brightness) differences or  
73 contrasts between a prey and its background (Troscianko *et al.* 2016); and those that  
74 quantify the complexity of the visual scene against which the prey is viewed (Xiao & Cuthill  
75 2016). Many of these are supported by empirical evidence demonstrating their efficacy in  
76 quantifying predation risk. However, while the application of these various metrics has  
77 made significant contributions to our understanding of the visual features that influence  
78 prey conspicuousness (Troscianko, Skelhorn & Stevens 2017), they tend to be employed  
79 independently, despite the fact that the visual features they encapsulate are typically  
80 available simultaneously to any animal viewing a scene. This limits our understanding of  
81 how these different visual features may be differentially weighted by a predator's visual  
82 system. Moreover, differences in the way these various metrics are implemented and the  
83 different assumptions they make (Troscianko, Skelhorn & Stevens 2017) means they are not  
84 easily combined into a holistic measure of signal conspicuousness, which is ultimately what  
85 choice is based on (Stevens & Merilaita 2009). One recent exception to this is the study by  
86 Xiao and Cuthill (2016), which used various measures of 'visual clutter' in the background  
87 against which prey were viewed to estimate detectability. Their approach allowed the  
88 relative efficacy of chromatic, achromatic and textural (i.e. orientation-based) clutter to be  
89 explored independently, but could also be combined into a composite measure that  
90 simultaneously considered clutter across all three feature types.

91 Here I describe an alternative approach, based on the neurophysiologically-inspired model  
92 of bottom-up visual attention described by Itti, Koch and Niebur (1998). The adaptation of  
93 this model described here allows the computation of species-relevant ‘saliency maps’, which  
94 topographically encode conspicuity over an entire visual scene and hence intrinsically  
95 incorporate the relative salience of both the target and its (heterogeneous) background. I  
96 then demonstrate that relative target salience is a good predictor of the performance of  
97 avian predators searching for camouflaged artificial prey both under constrained conditions  
98 in the lab, using Japanese quail (*Coturnix japonica*) searching for computer-generated  
99 targets on a computer screen, and in the field, using the predation of artificial moth-like  
100 targets by wild birds. In order to provide a comparison with other approaches that have  
101 successfully been used to characterise prey conspicuousness in comparable experiments, I  
102 also compare the performance of the saliency model described here with the best-  
103 performing models identified by Troscianko, Skelhorn and Stevens (2017) in their  
104 comprehensive comparison of models available at the time, and those used previously by  
105 Xiao and Cuthill (2016).

106

## 107 **Methods**

### 108 **Modelling visual salience**

109 In order to model the salience of features within a heterogeneous visual scene I adapt the  
110 model of bottom-up visual attention described by Itti, Koch and Niebur (1998). This model,  
111 and adaptations of it, are widely used within computer vision, neuroscience and human  
112 cognition (Itti & Koch 2001; Borji & Itti 2013), and have also been used to address questions  
113 in animal signalling (Peters 2010). Although many extensions to the model have been  
114 proposed in order to improve the fit to psychophysical data on human saliency perception  
115 (Borji & Itti 2013), the original version of the model still provides an excellent base from  
116 which to adapt the concept for non-human animals. For a full description of the underlying  
117 rationale and computation details readers are referred to Koch and Ullman (1985), Itti, Koch  
118 and Niebur (1998) and Walther and Koch (2006); here I provide an overview of the model  
119 architecture (Fig. 1), noting in particular where adaptations have been made to improve

120 generality and to address the specific question of target detection. Wherever possible,  
121 notation follows that used in Itti, Koch and Niebur (1998) for consistency.

122 The original model was inspired by the neurophysiological characteristics of human (and  
123 other trichromatic primate) visual systems, and so includes some assumptions that may not  
124 be appropriate for modelling saliency in other species. In particular, most applications of the  
125 model use an RGB image as input, in which each of the three colour channels (R, G and B) is  
126 assumed to broadly correspond to the response of one of the three cone classes in the  
127 human retina (Mollon 1989), and luminance is estimated as the mean of these three colour  
128 channels (Walther & Koch 2006). However, it is unlikely that these assumptions are  
129 appropriate for the majority of animal species (Osorio & Vorobyev 2005). In order to  
130 increase the generality of the model, I therefore adapted it to accept an arbitrary number of  
131  $n \times m$  grayscale ‘images’  $I$  as inputs, each of which is assumed to provide a topographical  
132 representation of the quantum catch of one of the viewing animal’s cone classes. In this  
133 paper I use birds as model predators (see below), and so the model was explicitly adapted  
134 for a tetrachromatic visual system in which four classes of single cone (long wavelength-,  
135 medium wavelength-, short wavelength- and ultraviolet/violet-sensitive, denoted L, M, S  
136 and U, respectively) are assumed to contribute to colour perception, and double cones (D)  
137 are assumed to contribute to luminance perception (Osorio, Miklosi & Gonda 1999; Jones &  
138 Osorio 2004; Osorio & Vorobyev 2005), although it would be straightforward to modify this  
139 to cope with variable numbers of cone classes (e.g. to represent dichromatic or  
140 pentachromatic visual systems) and different luminance perception mechanisms (e.g. those  
141 based on the summed input from two or more cone classes; Endler and Mielke (2005)).  
142 These input images are denoted  $I_L$ ,  $I_M$ ,  $I_S$ ,  $I_U$  and  $I_D$ , respectively.

143 For each of these input images, a Gaussian pyramid is then constructed by iteratively low-  
144 pass filtering and subsampling the image to produce a sequence of reduced-resolution  
145 images (Walther & Koch 2006). At each successive iteration, the next levels  $\sigma = [0, \dots, 7]$   
146 of the pyramid are obtained, such that the resolution of level  $\sigma$  is  $1/2^\sigma$  times the original  
147 image resolution; i.e., the seventh level has a resolution of 1/128th that of the input image.  
148 Each level of the pyramid is then further decomposed into a series of ‘maps’, corresponding  
149 to the early visual features of luminance, colour and orientation. For luminance, the local  
150 map at level  $\sigma$ ,  $M_L(\sigma)$ , is simply

$$M_L(\sigma) = I_D(\sigma). \quad (1)$$

151 The original model assumes that colour can be encoded using four broadly tuned colour  
 152 channels – namely red, green, blue and yellow (i.e. a linear combination of the red and  
 153 green channels) – and that local colour maps can be constructed on the basis of red–  
 154 green/green–red and blue–yellow/yellow–blue double opponent interactions (Livingstone &  
 155 Hubel 1984; Itti & Koch 2001; Walther & Koch 2006). However, while this may be  
 156 appropriate for the visual system of trichromatic primates on which the original model was  
 157 based, it is unlikely that these particular opponent interactions are appropriate for the  
 158 overwhelming majority of species (Kelber, Vorobyev & Osorio 2003). In this adaptation of  
 159 the model, rather than assume that colour perception results from specific opponent  
 160 interactions, I adopt a more general approach in which all possible pairwise colour  
 161 opponent interactions between the cone classes putatively contributing to colour  
 162 perception are considered (*sensu* Vorobyev and Osorio (1998)). Because birds are used  
 163 here, I therefore considered six putative opponent interactions: LM, LS, LU, MS, MU and SU,  
 164 although it would be straightforward to incorporate or restrict this to specific known or  
 165 hypothesised opponent interactions, if this information was available for the species under  
 166 study (e.g. Osorio, Miklosi and Gonda (1999)). Local colour maps are computed following  
 167 Walther and Koch (2006): for the putative LM opponent mechanism, for example, the  
 168 corresponding colour map  $M_{LM}(\sigma)$  at level  $\sigma$  is calculated as

$$M_{LM}(\sigma) = \frac{|I_L(\sigma) - I_M(\sigma)|}{I_D(\sigma)}. \quad (2)$$

169 Maps encoding for the putative LS, LU, MS, MU and SU mechanisms are created in a similar  
 170 way.

171 In the model it is assumed that textural (i.e. orientation-based) features are detected using  
 172 achromatic information (Itti & Koch 2001; Walther & Koch 2006). Local orientation maps  
 173  $M_\theta(\sigma)$  are therefore computed by convolving (Russ & Neal 2016, p. 352) the levels of the  $I_D$   
 174 pyramid with Gabor filters, such that

$$M_\theta(\sigma) = |I_D(\sigma) * G_0(\theta)| + |I_D(\sigma) * G_{\pi/2}(\theta)|, \quad (3)$$

175 where  $G_\psi(\theta)$  is a Gabor filter with a standard deviation of  $7/3$  pixels, a phase of  $\psi \in$   
 176  $\{0, \pi/2\}$  and an orientation of  $\theta \in \{0^\circ, 45^\circ, 90^\circ, 135^\circ\}$  (following Walther and Koch (2006)),  
 177 and  $*$  denotes convolution.

178 The next step is to construct a number of ‘feature maps’ that encode local luminance, colour  
 179 and orientation contrasts, using a set of linear ‘centre-surround’ operations analogous to  
 180 visual receptive fields (Hubel & Wiesel 1959). Typical visual neurons are most sensitive to a  
 181 small region of visual space (the centre), while stimuli presented in a broader antagonistic  
 182 region around the centre (the surround) inhibit the neural response. This increases  
 183 sensitivity to local spatial discontinuities, and so is particularly well-suited to detecting  
 184 regions of space which locally stand out from their surround (i.e. which are salient). Centre-  
 185 surround operations are implemented in the model as differences between a ‘centre’ fine  
 186 scale  $c$  and a ‘surround’ coarser scale  $s$ . Specifically, the centre is a pixel at scale  $c \in \{2,3,4\}$   
 187 and the surround is the corresponding pixel at scale  $s = c + \delta$ , where  $\delta \in \{3,4\}$ . Such  
 188 across-scale differences, denoted ‘ $\ominus$ ’ below, are obtained by interpolation to the finer scale  
 189 followed by point-by-point subtraction (Itti & Koch 2001). A feature map  $F$  for a particular  
 190 centre and surround is therefore calculated as

$$F_k(c, s) = N(|M_k(c) \ominus M_k(s)|), \quad (4)$$

191 where  $\forall k K \in \{L\} \cup \{LM, LS, LU, MS, MU, SU\} \cup \{0^\circ, 45^\circ, 90^\circ, 135^\circ\}$ , and  $N(\cdot)$  is an  
 192 iterative, nonlinear normalisation operator, simulating local competition between  
 193 neighbouring salient locations (Itti & Koch, 2001). The normalisation process is fully  
 194 described elsewhere (Itti, Koch & Niebur 1998; Walther & Koch 2006), but in brief each  
 195 feature map is normalised to the range  $[0,1]$  and then iteratively convolved by a two-  
 196 dimensional difference-of-Gaussian filter. Between iterations, the original image is added to  
 197 the new one and negative values set to zero. The effect of this is (i) to eliminate feature-  
 198 dependent differences caused by different feature extraction mechanisms, and (ii) to  
 199 promote regions of the map which differ most from the average (i.e. which are likely to be  
 200 the most salient), while suppressing homogenous or repetitive regions.

201 These feature maps are then combined into three ‘conspicuity maps’, for luminance  $C_L$ ,  
 202 colour  $C_C$ , and orientation  $C_O$  (Fig. 2), using across-scale addition (denoted ‘ $\oplus$ ’ below),

203 which consists of reduction of each map to scale  $\sigma = 4$  and point-by-point addition (Itti,  
 204 Koch & Niebur 1998), to give

$$C_L = N \left( \bigoplus_{c=2}^4 \bigoplus_{s=c+3}^{c+4} N(F_L(c, s)) \right), \quad (5)$$

$$C_C = N \left( \bigoplus_{c=2}^4 \bigoplus_{s=c+3}^{c+4} \sum_{\varphi \in \{LM, LS, LU, MS, MU, SU\}} N(F_\varphi(c, s)) \right), \quad (6)$$

$$C_O = N \left( \sum_{\theta \in \{0^\circ, 45^\circ, 90^\circ, 135^\circ\}} N \left( \bigoplus_{c=2}^4 \bigoplus_{s=c+3}^{c+4} N(F_\theta(c, s)) \right) \right). \quad (7)$$

205 Finally, these three conspicuity maps are linearly combined to produce a single overall  
 206 saliency map  $S$  (Fig. 2), such that

$$S = \omega_L C_L + \omega_C C_C + \omega_O C_O, \quad (8)$$

207 where  $\omega_L$ ,  $\omega_C$  and  $\omega_O$  are weighting factors in the range  $[0,1]$ , that allow the three feature  
 208 types to contribute differentially to saliency. The resulting saliency map topographically  
 209 encodes conspicuity over the entire visual scene, and therefore provides a continuous  
 210 measure of salience at any given location.

211

## 212 **Computing target salience**

213 In order to identify the location of a relevant target (e.g. a prey item) in a visual scene, a  
 214 viewing animal must be able to distinguish the region containing the target of interest from  
 215 other (possibly equally) salient regions of the background (i.e. the signal must be sufficiently  
 216 large relative to the prevailing noise; Navalpakkam & Itti 2006). The more salient the  
 217 elements of the background (or the less salient the elements of the target) are, on average,  
 218 the harder this task will be. Quantifying the relative salience of a target therefore requires  
 219 calculating an appropriate measure of distance between the value of pixels within the target  
 220 and the value of pixels in the background (see Fig. 3). Because these pixel values can follow  
 221 any arbitrary distribution (and so metrics based on mean pixel values are not always  
 222 appropriate; Navalpakkam & Itti 2006), here I used a histogram-based method which  
 223 compares the empirical cumulative histograms of pixel saliency values for the target and its



224 background; a common technique in image analysis (Pal & Peters 2010) which is insensitive  
225 to the specific distributions of the data. Specifically, relative target salience  $S_t$  is found by  
226 taking the sum of differences between the cumulative histograms of pixel salience values for  
227 the background  $H_b$  and the target  $H_t$  in a given saliency map as

$$S_t = \frac{1}{N} \sum_{j=1}^N H_b(j) - H_t(j), \quad (9)$$

228 where each cumulative histogram is divided into  $N$  bins, where  $j \in \{1, 2, 3, \dots, N\}$ . Here  $N$   
229 was set to 100. If pixel values within one or more visual features of the target (e.g. in colour,  
230 luminance and/or orientation) are high compared to the background, then  $S_t$  will be high  
231 ( $\gg 0$ ) and locating the target is predicted to be relatively easy (e.g. Fig. 3a,b); if the target  
232 and background share many visual features in common, or if the pixel values of the  
233 background are high compared to the target, then  $S_t$  will be low ( $\approx 0$ ) and locating the target  
234 is predicted to be hard (e.g. Fig. 3c,d). This metric therefore defines a holistic measure of  
235 ‘target salience’, which takes into account the salience of both the target itself and the  
236 salience of features within the background it is viewed against.

237 The implementation of the saliency model used here is based on a Matlab (MathWorks,  
238 Natick, MA) version of Itti, Koch and Niebur (1998)’s original model (Harel, Koch & Perona  
239 2006), adapted as described above, and available from [github.com/thomaswp/relative-saliency](https://github.com/thomaswp/relative-saliency).

240

## 241 **Predation experiments**

242 In order to test whether the model is able to predict the behaviour of real animals searching  
243 for targets that varied in their relative salience, I conducted two experiments in which avian  
244 predators were tasked with searching for and locating camouflaged artificial prey.

245 Experiment 1 was run under controlled conditions in the lab, using Japanese quail (*Coturnix*  
246 *japonica*) searching for computer-generated targets on a computer screen. Experiment 2  
247 was conducted in the field, employing a widely used approach (Cuthill *et al.* 2005) to  
248 quantify the detection of artificial targets by wild birds. In both cases, targets consisted of  
249 moth-like patterned triangles, viewed against a bark background. The visual scene in which  
250 each of the prey targets was viewed (either the computer screen, or calibrated photographs  
251 of the targets in situ in the field) was then used to construct the five quantum catch ‘images’

252 needed for the computation of target salience. Full methodological details of these  
253 experiments are given in the supplementary material.

254

### 255 **Comparison with alternative metrics**

256 A large number of metrics have been developed to characterise prey conspicuousness,  
257 many of which have been very successful in predicting predator performance across a range  
258 of species and contexts. Here I provide a qualitative comparison of the performance of the  
259 saliency model described in this paper with some of these other approaches. However,  
260 rather than exhaustively test every available metric (not least because such a comparison  
261 has recently been conducted; Troscianko, Skelhorn and Stevens (2017)), here I focus  
262 specifically on the best-performing metrics identified by Troscianko, Skelhorn and Stevens  
263 (2017) that take into account both the characteristics of the target and the characteristics of  
264 its background (and so provide a meaningful comparison with the saliency model described  
265 here), along with the visual ‘clutter’ metrics used in the recent paper by Xiao and Cuthill  
266 (2016). These metrics are listed in Table 1, summarised in the supplementary material and  
267 described in detail in the original publications (Rosenholtz *et al.* 2005; Stevens & Cuthill  
268 2006; Stoddard, Kilner & Town 2014; Xiao & Cuthill 2016; Troscianko, Skelhorn & Stevens  
269 2017).

270

### 271 **Statistical analysis**

272 To test whether target salience predicted predator success in the two experiments, I used  
273 (generalised) linear mixed-effect models, fitted using the ‘lmer’ and ‘glmer’ functions in the  
274 ‘lme4’ package (Bates *et al.* 2015) for R version 3.3.1. Full details are given in the  
275 supplementary material. In each case significance was determined by comparing a full  
276 model to models lacking the effect of interest using likelihood ratio tests (Crawley 2005),  
277 and assumptions validated following Zuur, Ieno and Elphick (2010).

278 Because the relative contribution of the different feature types (luminance, colour and  
279 orientation) to the perception of overall salience is unknown for birds (Xiao & Cuthill 2016),  
280 target salience was initially calculated from saliency maps in which each conspicuity map  
281 was weighted equally (i.e.  $\omega_L = \omega_C = \omega_O = 1$  in Eq. 8). However, it is unlikely that animals

282 do in fact weight these different features equally (Rosenholtz *et al.* 2005), and so it is useful  
283 to explore which set of feature weights provides the best predictive power. To do this, I  
284 systematically varied the values of  $\omega_L$ ,  $\omega_C$  and  $\omega_O$  in the computation of the final saliency  
285 map, and then reran the analyses for each combination of weights. In each case, the quality  
286 of the model fit was quantified using its AIC score, with the ‘optimal’ combination of weights  
287 defined as those which resulted in the lowest AIC (Burnham & Anderson 2002). For ease of  
288 comparison, AIC scores are presented as differences from this smallest AIC (i.e. in terms of  
289 their  $\Delta$ AIC; Burnham & Anderson 2002).

290 In order to compare the relative performance of the saliency model described here with the  
291 various alternative metrics, each of the analyses was rerun, but substituting ‘target salience’  
292 for each of the alternative metrics in turn. The quality of the model fit in each case was  
293 quantified using its  $\Delta$ AIC score, as above, allowing qualitative comparison between the  
294 metrics. Models were considered equally well-fitting if  $\Delta$ AIC < 2 (Burnham & Anderson  
295 2002).

296

## 297 **Results**

### 298 **Experiment 1**

299 For quail predating virtual moths the time taken to catch camouflaged prey was significantly  
300 predicted by the salience of the target ( $\chi^2(1) = 19.77$ ,  $p < 0.001$ ), with time taken decreasing  
301 as the target became increasingly salient (Fig. 4a). There was no evidence of predator  
302 learning over successive trials ( $\chi^2(1) = 0.17$ ,  $p = 0.680$ ), or any evidence that prey nearer the  
303 centre of the screen were quicker to catch ( $\chi^2(1) = 0.11$ ,  $p = 0.740$ ). However, assuming that  
304 the visual features contributing to target salience were equally weighted (i.e.  $\omega_L = \omega_C =$   
305  $\omega_O = 1$ ) did not produce the best-fitting model (Fig. 4b-d); instead, model fit increased  
306 roughly linearly as the relative luminance ( $\omega_L$ ) and orientation ( $\omega_O$ ) weights increased (Fig.  
307 4b), with a moderate contribution from colour ( $\omega_C$ ) (Fig. 4c,d). The best-fitting model had  
308 the following feature weights:  $\omega_L = 1.0$ ,  $\omega_C = 0.5$  and  $\omega_O = 0.7$  ( $\chi^2(1) = 20.38$ ,  $p < 0.001$ ).

309 Comparing the alternative camouflage metrics, the best-fitting models were the ‘optimally’-  
310 weighted ( $\Delta$ AIC = 0.0) and equally-weighted ( $\Delta$ AIC = 0.9) saliency models, both of which

311 provided a substantially better fit than the next best metric, the Gabor Edge Disruption  
312 Ratio ( $\Delta AIC = 10.6$ ) (Table 1).

313

## 314 **Experiment 2**

315 Target salience significantly predicted the survival of moth-like targets deployed in the field  
316 ( $\chi^2(1) = 8.93$ ,  $p = 0.003$ ), such that those surviving predation by birds had a significantly  
317 lower target salience than those that were predated (Fig. 5a). As for Experiment 1, model fit  
318 varied considerably with feature weight, although the overall pattern was somewhat  
319 different. Specifically, the best-fitting model occurred when orientation was weighted high  
320 ( $\omega_o = 0.9$ ), luminance was weighted relatively low ( $\omega_L = 0.3$ ), and colour did not  
321 contribute at all to target salience ( $\omega_c = 0.0$ ) ( $\chi^2(1) = 18.56$ ,  $p < 0.001$ ; Fig. 5b,c,d).

322 When comparing between the different metrics, the best-fitting models were those  
323 including Sub-band Entropy ( $\Delta AIC = 0.0$ ) and the 'optimally'-weighted saliency model ( $\Delta AIC =$   
324  $1.5$ ). The next-best fitting models included Luminance Feature Congestion ( $\Delta AIC = 4.8$ ), the  
325 equally-weighted saliency model ( $\Delta AIC = 11.2$ ), Overall Feature Congestion ( $\Delta AIC = 11.4$ ) and  
326 Orientation Congestion ( $\Delta AIC = 11.8$ ) (Table 1).

327

## 328 **Discussion**

329 This study explored the efficacy of species-relevant saliency maps as predictors of predator  
330 performance in two tasks involving locating cryptic targets against noisy backgrounds. The  
331 results clearly demonstrate that across both laboratory and field contexts target salience is a  
332 good predictor of predator performance, with laboratory quail locating salient virtual moths  
333 quicker than those that were estimated to appear less salient (Experiment 1), and wild birds  
334 most successfully predated artificial moths that were deemed the most salient (Experiment  
335 2). Moreover, it allowed information on the possible weighting of the different feature types  
336 contributing to a predator's perception of target salience to be inferred. Interestingly, these  
337 weightings differed between the two experiments. In Experiment 1, birds appeared to be  
338 using a combination of luminance, colour and orientation features to inform their  
339 behaviour, although the highest weightings came from luminance and orientation. In

340 Experiment 2, the birds appeared to be predominantly using orientation features, with a  
341 lesser reliance on luminance and no contribution at all from colour. While this provides  
342 some evidence that the relative efficacy of luminance-based cues may be greater than  
343 chromatic cues (Stevens and Cuthill (2006); cf. Schaefer and Stobbe (2006)), it is impossible  
344 to know whether the difference in the relative weightings of the three feature types  
345 between the two experiments was driven by differences in vision or cognition between the  
346 species involved, or by differences between the experimental setups. For example, in  
347 Experiment 2 the distance at which prey were viewed was likely to be both initially greater  
348 and considerably more variable than in Experiment 1, which would be important if the  
349 weighting of the different feature types depended on distance or perceived prey size.  
350 Moreover, the search space in Experiment 2 included three-dimensional information  
351 (providing a possible explanation for the reduced reliance of luminance cues, as these may  
352 be less useful when searching in a three-dimensional environment; Zhang *et al.* (2010)), and  
353 would have included elevated (but unmeasured) noise in luminance and colour due to  
354 short-term illumination changes, possibly rendering colour and luminance cues less reliable.  
355 However, despite these differences the findings of both experiments are broadly consistent  
356 with previous studies, in which the textural (i.e. orientation-based) complexity of the  
357 background (Xiao & Cuthill 2016) and the conspicuousness of the prey's outline (Stevens &  
358 Cuthill 2006; Lovell *et al.* 2013; Webster *et al.* 2013; Kang *et al.* 2015; Troscianko *et al.* 2016;  
359 Troscianko, Skelhorn & Stevens 2017) have been identified as important determinants of  
360 predator success. Orientation features therefore appear to be a key component in the  
361 detection of camouflaged prey across a range of species and contexts, although the results  
362 of this study emphasise the need to also consider the relative contribution of other feature  
363 types if we are to fully understand the mechanisms predators use to detect prey.

364 As well as predicting predator performance in the two experiments reported here, the  
365 performance of the saliency model also compared very favourably with a number of  
366 alternative metrics that have been proposed to quantify prey conspicuousness in analogous  
367 situations (Xiao & Cuthill 2016; Troscianko, Skelhorn & Stevens 2017). In Experiment 1 it  
368 performed substantially better than all the other metrics tested, possibly because the birds  
369 appeared to be using a combination of luminance, colour and orientation features to inform  
370 their behaviour; something that is not encapsulated in metrics that focus on a single feature

371 type. For example, the next best performing metric, the Gabor Edge Disruption Ratio, was  
372 found to perform extremely well in Troscianko, Skelhorn and Stevens (2017)'s human-based  
373 study, possibly because achromatic stimuli were used. While focussing on achromatic  
374 stimuli was entirely reasonable, given that the luminance channel in primates has numerous  
375 oriented edge detectors suitable for shape processing (Hesse & Georgeson 2005), colour is  
376 also known to contribute to target detection by facilitating the segregation of surfaces that  
377 differ in chromaticity (Gegenfurtner & Rieger 2000). It is possible, therefore, that had  
378 chromatic information also been unavailable in the present study, birds may have weighted  
379 orientation-based features more heavily. In Experiment 2, the best-performing metrics were  
380 Sub-band Entropy (cf. Xiao and Cuthill (2016)) and the 'optimally'-weighted saliency model,  
381 with Luminance Congestion also performing well. Such variation in model fit between the  
382 various metrics is likely to stem, at least in part, from what they are actually quantifying, as  
383 well as the characteristics of the specific prey and backgrounds used. For example, the  
384 'congestion' and 'clutter' metrics (which include Sub-band Entropy and Luminance  
385 Congestion) are global measures of the background against which the prey is viewed, and  
386 do not explicitly compare features of the prey with those of its background (Xiao & Cuthill  
387 2016). As such, a plain prey item against a congested background could actually appear  
388 highly salient. Similarly, other metrics focussing specifically on the outline of the prey, such  
389 as the number of true edges detected by the Hough transform (Stevens & Cuthill 2006) and  
390 the Gabor Edge Disruption Ratio (Troscianko, Skelhorn & Stevens 2017), ignore at least  
391 some of the prey's internal features, which may themselves be highly salient. Further work  
392 is therefore needed to identify the strengths and weaknesses of these various approaches  
393 across different contexts, particularly with regard to the alternative mechanisms of  
394 camouflage (Stevens & Merilaita 2009). For example, the relative performance of the edge-  
395 based metrics may well have been improved if the targets explicitly incorporated disruptive  
396 patterns rather than simply representing samples of the background. It should also be noted  
397 that, while the saliency model performed well, measures of overall salience per se tell us  
398 little about the mechanisms underpinning successful camouflage. To address this, we still  
399 need to consider the various component parts separately.

400 The model of visual salience used in this paper is primarily concerned with 'bottom-up'  
401 salience, which reflexively directs visual focus based on certain low-level visual features (Itti

402 & Koch 2001). This mimics the case where a predator has no a priori knowledge of the prey  
403 or its background, and is not an unrealistic assumption for the experiments described here  
404 given that each of the moths and background combinations was unique. However, given  
405 repeated exposure to a prey item with particular identifying characteristics, a predator may  
406 have the opportunity to learn about the statistical properties of both the prey and its  
407 background and use this to optimise its search (Navalpakkam & Itti 2006; Borji & Itti 2013).  
408 A camouflaged prey item that lacks bottom-up salience could therefore still be effectively  
409 detected through 'top-down', or knowledge-based, guidance to known prey locations and  
410 features. In terms of the model used here, this could be implemented by optimising the  
411 weighting given to each of the bottom-up feature and conspicuity maps when computing  
412 the final saliency map, with the aim of giving high weighting to features predominantly  
413 found in prey and low weighting to features that predominate in the background. This  
414 would be akin to a sensory system enhancing neurons tuned to properties of the prey  
415 and/or suppressing neurons tuned to properties of the background, thereby maximising  
416 target detection speed (Navalpakkam & Itti 2006).

417 The focus of this paper has been on using salience to describe the efficacy of camouflage in  
418 animals. However, the general approach would apply equally well to the assessment of  
419 conspicuity in animals or plants that have evolved to maximise their probability of  
420 detection, including those displaying conspicuous signals within a mate choice context.  
421 Because it is possible to use the feature and (colour, luminance and orientation) conspicuity  
422 maps to make inferences about which feature channel most contributes to the saliency of a  
423 target, it may allow us to better understand both signal design and receiver cognition. For  
424 example, Fig. 6 shows the three peafowl-specific conspicuity maps derived from a calibrated  
425 colour image of a displaying peacock (*Pavo cristatus*), in which the relative contribution of  
426 colour, luminance and orientation features are presented. There is little evidence of  
427 luminance salience in the elements of the peacock's colouration compared to the  
428 background they are viewed against (although this may be because saliency was derived  
429 from a static photograph; due to the iridescence of the peacock's eyespots [Loyau *et al.*  
430 2007], there is likely to be large modulations of luminance with movement, creating salience  
431 through signal change). However, the eyespots on the tail feathers, which have been  
432 repeatedly implicated as a target for female choice (Petrie, Halliday & Sanders 1991; Petrie

433 & Halliday 1994; Loyau *et al.* 2007; Dakin & Montgomerie 2011), exhibit clear colour  
434 salience when viewed against their local background, with the different colour elements of  
435 the eyespots clearly delineated. Furthermore, the radial changes in the tail feather  
436 orientation around the train result in local orientation contrasts and hence regions of high  
437 orientation salience. Combined, these make elements of the peacock's train highly salient  
438 against their local background. This is, of course, simply an illustrative example; however, an  
439 approach like this could allow studies to identify and focus on particular aspects of a signal  
440 that contribute disproportionately to its conspicuousness, while avoiding aspects that may  
441 be poorly perceived.

442 In this study the focus was necessarily on avian visual systems under fairly constrained  
443 experimental conditions, although the visual salience of a given target may in fact differ  
444 considerably between receivers of different species and in response to variation in the  
445 physical and biological environment. In particular, the spectrum, intensity and orientation of  
446 illuminating light, as well as the presence of features such as shadows, will likely play a  
447 significant role in determining how salient a target appears. This has been widely explored  
448 in terms of chromatic contrasts (Uy & Endler 2004), although less so in terms of luminance  
449 and orientation (Troscianko *et al.* 2016). Moreover, several features which have been linked  
450 to salience in humans remain largely unexplored in animals, including contrasts arising from  
451 variation in depth (Zhang *et al.* 2012; Ma & Hang 2015) and motion (Belardinelli, Pirri &  
452 Carbone 2009; Peters 2010); the approach used here provides the flexibility needed to  
453 incorporate these different visual features (Walther & Koch 2006) to explore how salient  
454 targets appear to a variety of different visual systems, across a range of different biological  
455 and physical contexts.

456

## 457 **Acknowledgements**

458 I thank Oliver Burman and Charles Deeming for valuable discussions, and Innes Cuthill,  
459 Martin Stevens and an anonymous reviewer for comments that greatly improved the  
460 manuscript. This work was supported in part by a Natural Environment Research Council  
461 fellowship (NE/F016514/1).

462



## 463 **Data Accessibility**

464 Data associated with this paper is available from [eprints.lincoln.ac.uk/31393](http://eprints.lincoln.ac.uk/31393).

465

## 466 **References**

- 467 Bates, D., Machler, M., Bolker, B.M. & Walker, S.C. (2015) Fitting linear mixed-effects  
468 models using lme4. *Journal of Statistical Software*, **67**, 1-48.
- 469 Belardinelli, A., Pirri, F. & Carbone, A. (2009) Motion Saliency Maps from Spatiotemporal  
470 Filtering. *Attention in Cognitive Systems*, **5395**, 112-123.
- 471 Borji, A. & Itti, L. (2013) State-of-the-Art in Visual Attention Modeling. *Ieee Transactions on*  
472 *Pattern Analysis and Machine Intelligence*, **35**, 185-207.
- 473 Burnham, K.P. & Anderson, D.R. (2002) *Model Selection and Multimodel Inference: A*  
474 *Practical Information-Theoretic Approach*, 2nd ed. edn. Springer-Verlag.
- 475 Chiao, C.C., Chubb, C., Buresch, K., Siemann, L. & Hanlon, R.T. (2009) The scaling effects of  
476 substrate texture on camouflage patterning in cuttlefish. *Vision Research*, **49**, 1647-  
477 1656.
- 478 Crawley, M.J. (2005) *Statistics: an introduction using R*. John Wiley, Chichester, UK.
- 479 Cuthill, I.C., Stevens, M., Sheppard, J., Maddocks, T., Parraga, C.A. & Troscianko, T.S. (2005)  
480 Disruptive coloration and background pattern matching. *Nature*, **434**, 72-74.
- 481 Dakin, R. & Montgomerie, R. (2011) Peahens prefer peacocks displaying more eyespots, but  
482 rarely. *Animal Behaviour*, **82**, 21-28.
- 483 Dimitrova, M. & Merilaita, S. (2014) Hide and seek: properties of prey and background  
484 patterns affect prey detection by blue tits. *Behavioral Ecology*, **25**, 402-408.
- 485 Endler, J.A. & Mielke, P.W. (2005) Comparing entire colour patterns as birds see them.  
486 *Biological Journal of the Linnean Society*, **86**, 405-431.
- 487 Frey, H.P., Wirz, K., Willenbockel, V., Betz, T., Schreiber, C., Troscianko, T. & Konig, P. (2011)  
488 Beyond correlation: do color features influence attention in rainforest? *Frontiers in*  
489 *Human Neuroscience*, **5**.
- 490 Gegenfurtner, K.R. & Rieger, J. (2000) Sensory and cognitive contributions of color to the  
491 recognition of natural scenes. *Current Biology*, **10**, 805-808.
- 492 Godfrey, D., Lythgoe, J.N. & Rumball, D.A. (1987) Zebra Stripes and Tiger Stripes - the  
493 Spatial-Frequency Distribution of the Pattern Compared to That of the Background Is  
494 Significant in Display and Crypsis. *Biological Journal of the Linnean Society*, **32**, 427-  
495 433.
- 496 Harel, J., Koch, C. & Perona, P. (2006) Graph-based visual saliency. *Advances in neural*  
497 *information processing systems*, pp. 545-552.
- 498 Hart, N.S. (2002) Vision in the peafowl (*Aves: Pavo cristatus*). *Journal of Experimental*  
499 *Biology*, **205**, 3925-3935.
- 500 Hesse, G.S. & Georgeson, M.A. (2005) Edges and bars: where do people see features in 1-D  
501 images? *Vision Research*, **45**, 507-525.
- 502 Hubel, D.H. & Wiesel, T.N. (1959) Receptive fields of single neurones in the cat's striate  
503 cortex. *Journal of Physiology*, **124**, 574-591.
- 504 Itti, L. & Koch, C. (2001) Computational modelling of visual attention. *Nature Reviews*  
505 *Neuroscience*, **2**, 194-203.

- 506 Itti, L., Koch, C. & Niebur, E. (1998) A model of saliency-based visual attention for rapid  
507 scene analysis. *Ieee Transactions on Pattern Analysis and Machine Intelligence*, **20**,  
508 1254-1259.
- 509 Jones, C.D. & Osorio, D. (2004) Discrimination of oriented visual textures by poultry chicks.  
510 *Vision Research*, **44**, 83-89.
- 511 Kang, C., Stevens, M., Moon, J.Y., Lee, S.I. & Jablonski, P.G. (2015) Camouflage through  
512 behavior in moths: the role of background matching and disruptive coloration.  
513 *Behavioral Ecology*, **26**, 45-54.
- 514 Kelber, A., Vorobyev, M. & Osorio, D. (2003) Animal colour vision - behavioural tests and  
515 physiological concepts. *Biological Reviews*, **78**, 81-118.
- 516 Kesner, R.P. & Olton, D.S. (2014) *Neurobiology of Comparative Cognition*. Psychology Press,  
517 New York, NY.
- 518 Koch, C. & Ullman, S. (1985) Shifts in Selective Visual-Attention - Towards the Underlying  
519 Neural Circuitry. *Human Neurobiology*, **4**, 219-227.
- 520 Livingstone, M.S. & Hubel, D.H. (1984) Anatomy and Physiology of a Color System in the  
521 Primate Visual-Cortex. *Journal of Neuroscience*, **4**, 309-356.
- 522 Lovell, P.G., Ruxton, G.D., Langridge, K.V. & Spencer, K.A. (2013) Egg-Laying Substrate  
523 Selection for Optimal Camouflage by Quail. *Current Biology*, **23**, 260-264.
- 524 Loyau, A., Gomez, D., Moureau, B.T., They, M., Hart, N.S., Saint Jalme, M., Bennett, A.T.D. &  
525 Sorci, G. (2007) Iridescent structurally based coloration of eyespots correlates with  
526 mating success in the peacock. *Behavioral Ecology*, **18**, 1123-1131.
- 527 Ma, C.Y. & Hang, H.M. (2015) Learning-based saliency model with depth information.  
528 *Journal of Vision*, **15**.
- 529 Merilaita, S. (2003) Visual background complexity facilitates the evolution of camouflage.  
530 *Evolution*, **57**, 1248-1254.
- 531 Navalpakkam, V. & Itti, L. (2006) An integrated model of top-down and bottom-up attention  
532 for optimizing detection speed. *2006 IEEE Computer Society Conference on Computer  
533 Vision and Pattern Recognition (CVPR'06)*, pp. 2049-2056.
- 534 Osorio, D., Miklosi, A. & Gonda, Z. (1999) Visual ecology and perception of coloration  
535 patterns by domestic chicks. *Evolutionary Ecology*, **13**, 673-689.
- 536 Osorio, D. & Vorobyev, M. (2005) Photoreceptor spectral sensitivities in terrestrial animals:  
537 adaptations for luminance and colour vision. *Proceedings of the Royal Society B-  
538 Biological Sciences*, **272**, 1745-1752.
- 539 Osorio, D. & Vorobyev, M. (2008) A review of the evolution of animal colour vision and  
540 visual communication signals. *Vision Research*, **48**, 2042-2051.
- 541 Pal, S.K. & Peters, J.F. (2010) *Rough Fuzzy Image Analysis: Foundations and Methodologies*.  
542 CRC Press, Boca Raton, FL.
- 543 Peters, R.A. (2010) Movement-based signalling and the physical world: modelling the  
544 changing perceptual task for receivers. *Modelling perception with artificial neural  
545 networks* (eds C.R. Tosh & G.D. Ruxton), pp. 269-292. Cambridge University Press,  
546 Cambridge.
- 547 Petrie, M. & Halliday, T. (1994) Experimental and Natural Changes in the Peacocks (Pavo  
548 Cristatus) Train Can Affect Mating Success. *Behavioral Ecology and Sociobiology*, **35**,  
549 213-217.
- 550 Petrie, M., Halliday, T. & Sanders, C. (1991) Peahens Prefer Peacocks with Elaborate Trains.  
551 *Animal Behaviour*, **41**, 323-331.

552 Rosenholtz, R., Li, Y., Mansfield, J. & Jin, Z. (2005) Feature congestion: a measure of display  
553 clutter. *Proceedings of the SIGCHI conference on human factors in computing*  
554 *systems, ACM*, pp. 761-770.

555 Russ, J.C. & Neal, F.B. (2016) *The Image Processing Handbook*, 7th edn. Taylor & Francis,  
556 Boca Raton, FL.

557 Ruxton, G.D., Sherratt, T.N. & Speed, M.P. (2004) *Avoiding Attack*. Oxford University Press,  
558 Oxford, UK.

559 Schaefer, H.M. & Stobbe, N. (2006) Disruptive coloration provides camouflage independent  
560 of background matching. *Proceedings of the Royal Society B-Biological Sciences*, **273**,  
561 2427-2432.

562 Spottiswoode, C.N. & Stevens, M. (2010) Visual modeling shows that avian host parents use  
563 multiple visual cues in rejecting parasitic eggs. *Proceedings of the National Academy*  
564 *of Sciences of the United States of America*, **107**, 8672-8676.

565 Stevens, M. & Cuthill, I.C. (2006) Disruptive coloration, crypsis and edge detection in early  
566 visual processing. *Proceedings of the Royal Society B*, **273**, 2141-2147.

567 Stevens, M. & Merilaita, S. (2009) Animal camouflage: current issues and new perspectives.  
568 *Philosophical Transactions of the Royal Society B-Biological Sciences*, **364**, 423-427.

569 Stoddard, M.C., Kilner, R.M. & Town, C. (2014) Pattern recognition algorithm reveals how  
570 birds evolve individual egg pattern signatures. *Nature Communications*, **5**, 4117.

571 They, M. & Casas, J. (2002) Predator and prey views of spider camouflage - Both hunter and  
572 hunted fail to notice crab-spiders blending with coloured petals. *Nature*, **415**, 133-  
573 133.

574 Troscianko, J., Skelhorn, J. & Stevens, M. (2017) Quantifying camouflage: how to predict  
575 detectability from appearance. *BMC Evolutionary Biology*, **17**, 7.

576 Troscianko, J., Wilson-Aggarwal, J., Stevens, M. & Spottiswoode, C.N. (2016) Camouflage  
577 predicts survival in ground-nesting birds. *Scientific Reports*, **6**.

578 Uy, J.A.C. & Endler, J.A. (2004) Modification of the visual background increases the  
579 conspicuousness of golden-collared manakin displays. *Behavioral Ecology*, **15**, 1003-  
580 1010.

581 Vorobyev, M. & Osorio, D. (1998) Receptor noise as a determinant of colour thresholds.  
582 *Proceedings of the Royal Society B*, **265**, 351-358.

583 Walther, D. & Koch, C. (2006) Modeling attention to salient proto-objects. *Neural Networks*,  
584 **19**, 1395-1407.

585 Webster, R.J., Hassall, C., Herdman, C.M., Godin, J.G.J. & Sherratt, T.N. (2013) Disruptive  
586 camouflage impairs object recognition. *Biology Letters*, **9**.

587 Xiao, F. & Cuthill, I.C. (2016) Background complexity and the detectability of camouflaged  
588 targets by birds and humans. *Proceedings of the Royal Society B*, **283**, 20161527.

589 Zhang, H.L., Lei, J.J., Fan, X.H., Wu, M.M., Zhang, P. & Bu, S.P. (2012) Depth Combined  
590 Saliency Detection Based on Region Contrast Model. *Proceedings of 2012 7th*  
591 *International Conference on Computer Science & Education, Vols I-Vi*, 763-766.

592 Zhang, Y., Jiang, G.Y., Yu, M. & Chen, K. (2010) Stereoscopic Visual Attention Model for 3D  
593 Video. *Advances in Multimedia Modeling, Proceedings*, **5916**, 314-324.

594 Zuur, A.F., Ieno, E.N. & Elphick, C.S. (2010) A protocol for data exploration to avoid common  
595 statistical problems. *Methods in Ecology and Evolution*, **1**, 3-14.

596

597

598 Table 1. Relative performance of the various metrics used to quantify target  
 599 conspicuousness, in terms of their  $\Delta AIC$ . Please refer to the supplementary material for a  
 600 full description of these metrics and details of the analysis. For each experiment, the best-  
 601 fitting model is denoted by an asterisk (\*).

Predictor	$\Delta AIC$ (Experiment 1)	$\Delta AIC$ (Experiment 2)
This Model (equal weighting of feature types)	0.9	11.2
This Model ('optimal' weighting of feature types)	0.0*	1.5
Gabor Edge Disruption Ratio	10.6	20.0
Number of SIFT Feature Correspondences	27.4	18.3
Colour Congestion	17.2	18.9
Luminance Congestion	16.7	4.8
Orientation Congestion	19.0	11.8
Overall Feature Congestion	19.0	11.4
Sub-band Entropy	20.3	0.0*
Number of Hough Edges	23.6	18.9

602

603

604

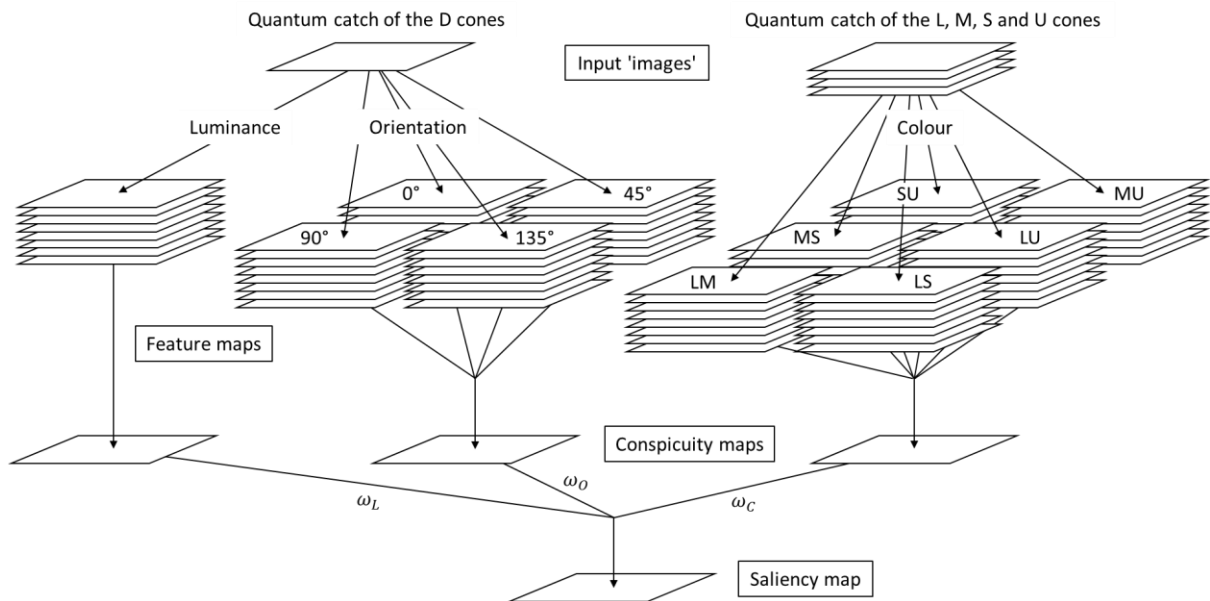
605

606

607

608

609



610

611 Figure 1. Schematic illustration of the saliency model used here, adapted from Itti, Koch and  
 612 Niebur (1998). Input to the model is a series of grayscale 'images', each representing  
 613 topographical variation in the estimated quantum catch of one of the viewing bird's cone  
 614 classes; one for each of the four single cones (L, M, S and U, which are assumed to  
 615 contribute to the perception of colour) and one for the double cones (D, which are assumed  
 616 to encode luminance). These are used to construct feature maps that encode local colour,  
 617 luminance and orientation contrasts, before being aggregated hierarchically, first by  
 618 grouping features by type into conspicuity maps, then by combining these conspicuity maps  
 619 (using the weights  $\omega_L$ ,  $\omega_C$  and  $\omega_O$ ) to compute the final saliency map. Please refer to the  
 620 text for full details.

621

622

623

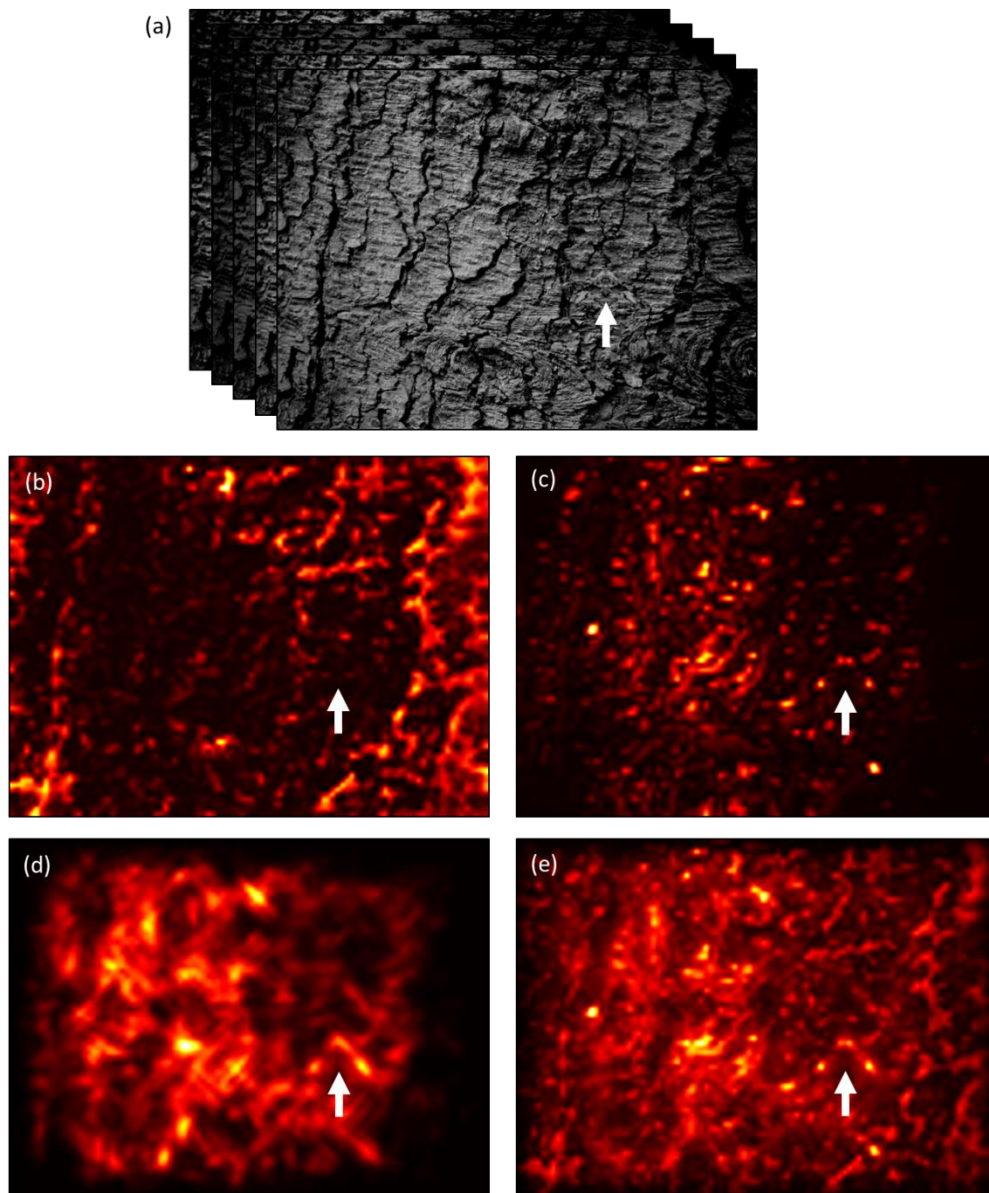
624

625

626

627

628



629

630 Figure 2. (a) Representative input ‘images’ for one of the stimuli used in Experiment 1.  
 631 These were used to compute conspicuity maps for (b) colour, (c) luminance and (d)  
 632 orientation, which were then combined (in this case using equal-weighting, i.e.  $\omega_L = \omega_C =$   
 633  $\omega_O = 1$ ) to produce the final saliency map (e). Please refer to the text for full details. In each  
 634 map, colour is proportional to salience, with lighter colours denoting regions of relatively  
 635 high salience and darker colours regions of relatively low salience. The camouflaged virtual  
 636 moth is shown by the white arrow, and is at the same corresponding position in each map.  
 637 In this example there is little evidence of colour salience in the target compared to its  
 638 background. However, some elements of the target’s pattern are relatively salient in the  
 639 luminance channel (seen as blobs of high salience corresponding to the positions of brighter  
 640 regions on the outer edge of the wings), and edges that differ in direction from the

641 surrounding background are clearly evident in the orientation channel. Combined, these  
642 features contribute to the overall salience of the target. Note that in each map the target is  
643 not necessarily the only (or most) salient region, but its salience is sufficiently high to likely  
644 make it conspicuous against this particular background to this particular predator.

645

646

647

648

649

650

651

652

653

654

655

656

657

658

659

660

661

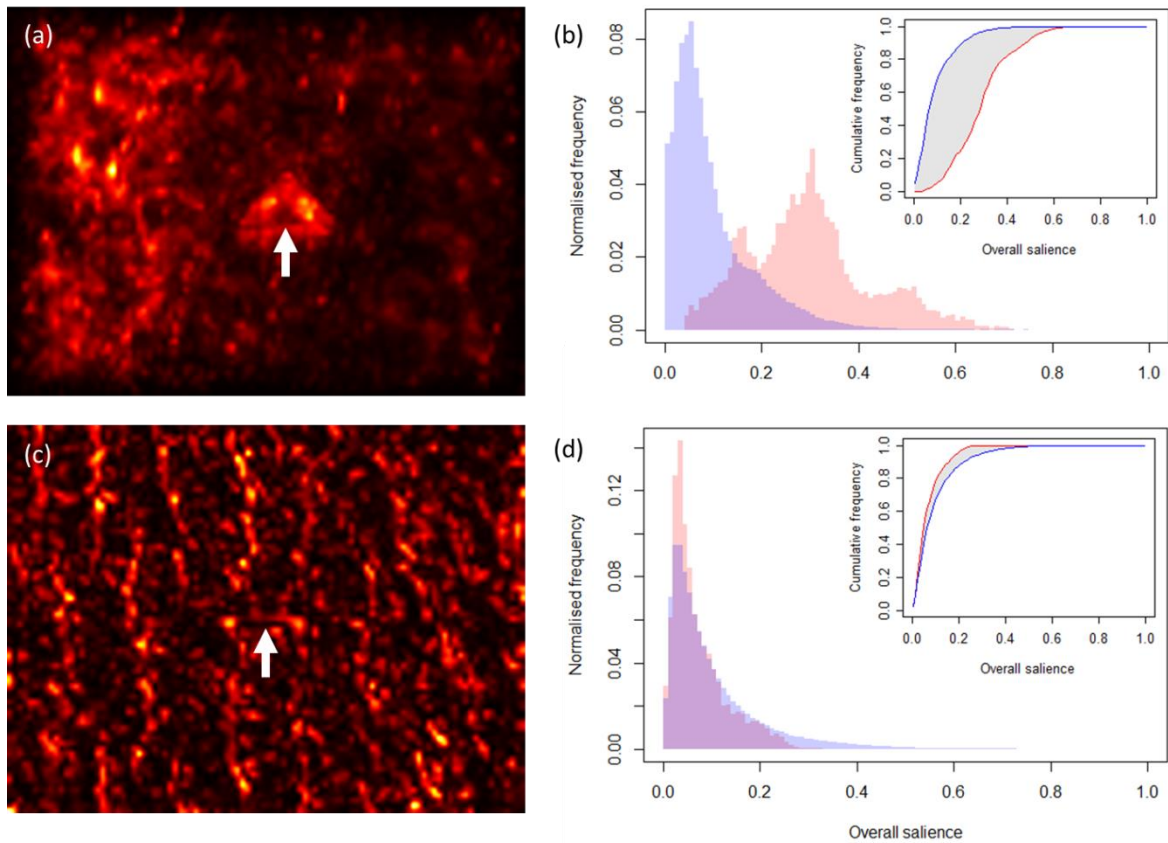
662

663

664

665

666



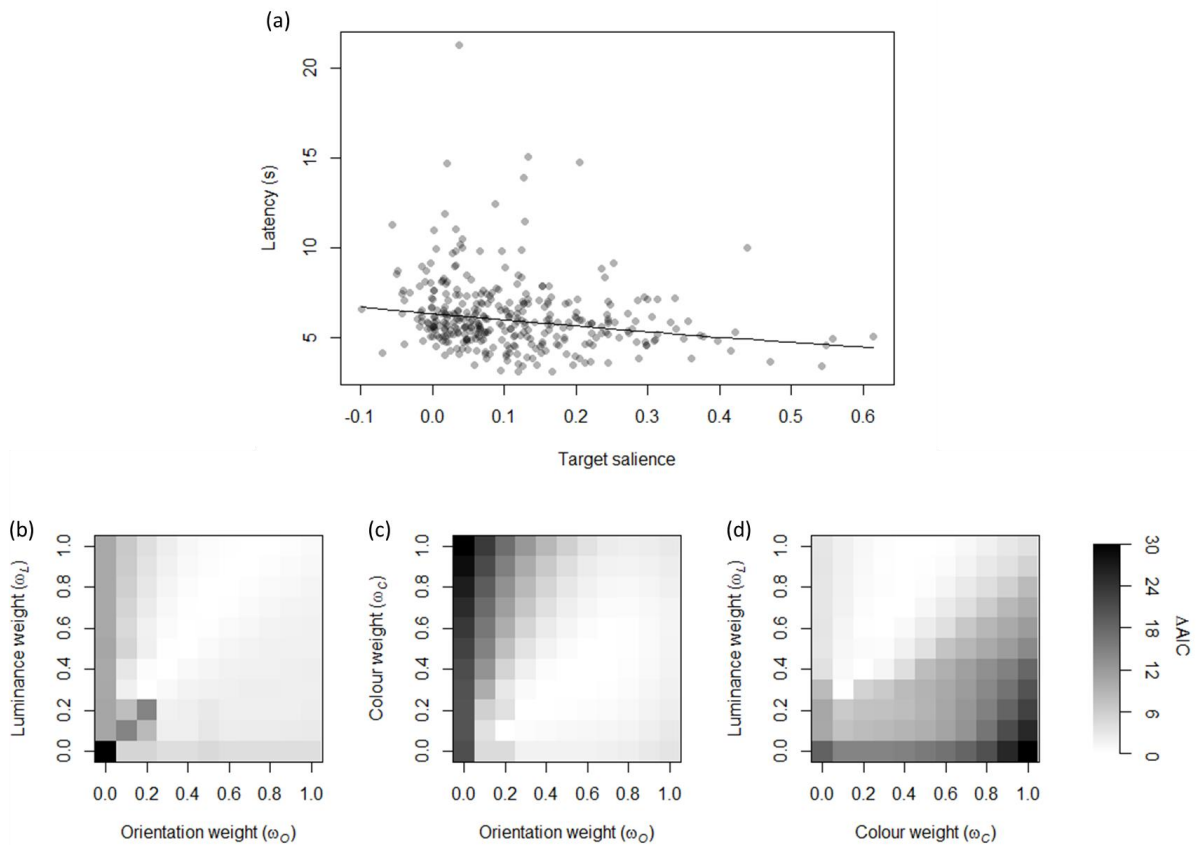
667

668 Figure 3. Calculation of target saliency, illustrated using representative stimuli from  
 669 Experiment 2. (a) Overall saliency map, which includes a relatively salient moth-like target  
 670 (indicated by the white arrow). Colour is proportional to saliency, with lighter colours  
 671 denoting regions of relatively high saliency and darker colours regions of relatively low  
 672 saliency. (b) Frequency histogram of pixel saliency values for the background (blue) and  
 673 target (red) of the scene shown in (a), with the region of overlap shown in purple. Both  
 674 histograms have been normalised to aid comparison. The inset shows the cumulative  
 675 histogram of these data, with the grey shaded region indicating the difference between  
 676 histograms from which relative target saliency was calculated. Please refer to the text for  
 677 full details. (c) Overall saliency map including a relatively unsalient moth-like target  
 678 (indicated by the white arrow), along with (d) the corresponding frequency and cumulative  
 679 histograms of pixel saliency values for the background (blue) and target (red).

680

681





682

683 Figure 4. (a) Time taken for Japanese quail to successfully predate virtual moths, as a  
 684 function of target salience. Each data point represents one moth, and data from all birds  
 685 have been combined for clarity. The solid line denotes the estimated fit from the linear  
 686 mixed-effects model. For simplicity, the three feature types (luminance, colour and  
 687 orientation) were assumed to contribute equally to the computation of target salience (i.e.  
 688  $\omega_L = \omega_C = \omega_O = 1$ ). (b-d) Variation in model  $\Delta AIC$  as the relative weight of the luminance,  
 689 colour and orientation features types was systematically changed. Grey values denote the  
 690 minimum  $\Delta AIC$  score for the given combination of weights, with lighter shades indicative of  
 691 better fitting models.

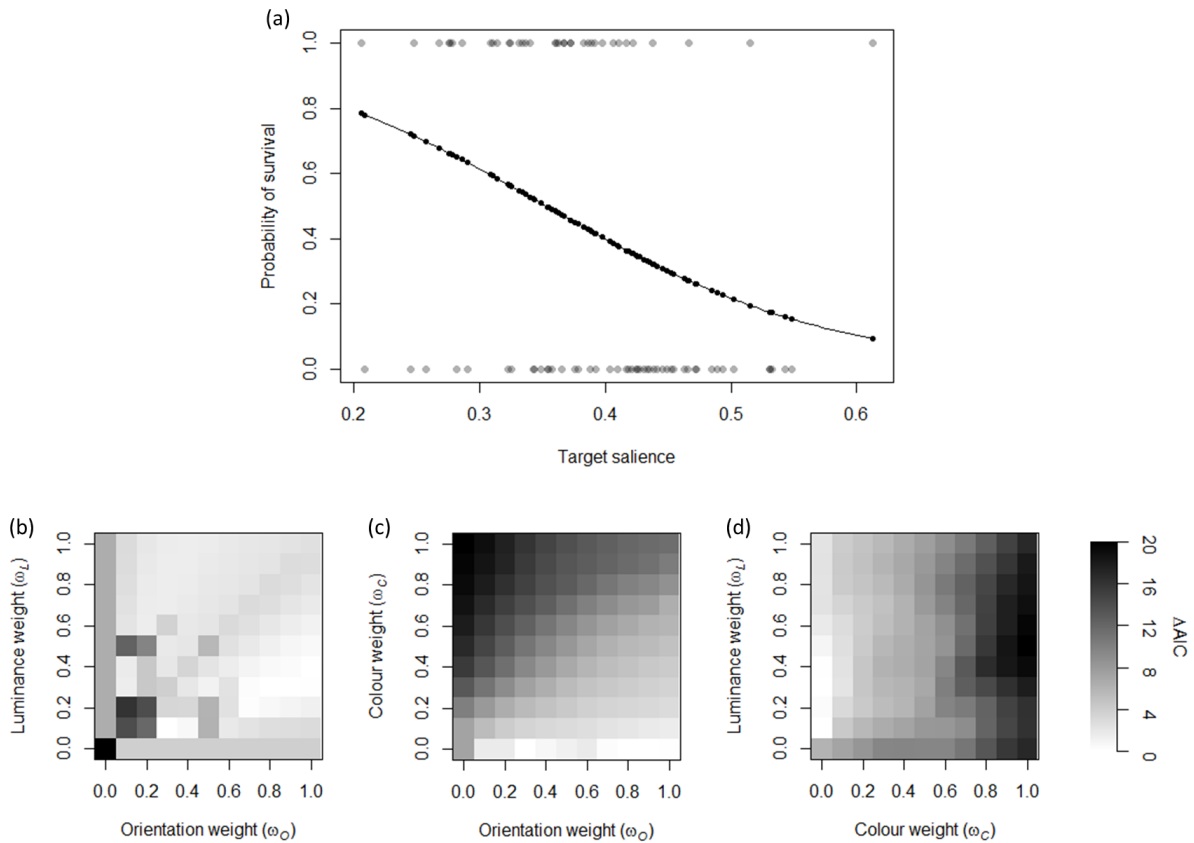
692

693

694

695

696



697

698 Figure 5. (a) The probability that moth-like targets survived predation by wild birds over a 24  
 699 hour period as a function of their salience. Individual data points represent a single target,  
 700 and the curve represents the fit of the binomial generalized linear mixed model used to  
 701 model the data. For simplicity, the three feature types (luminance, colour and orientation)  
 702 were assumed to contribute equally to the computation of target salience (i.e.  $\omega_L = \omega_C =$   
 703  $\omega_O = 1$ ). (b-d) Variation in model  $\Delta$ AIC as the relative weight of the luminance, colour and  
 704 orientation features types was systematically changed. Grey values denote the minimum  
 705  $\Delta$ AIC score for the given combination of weights, with lighter shades indicative of better  
 706 fitting models.

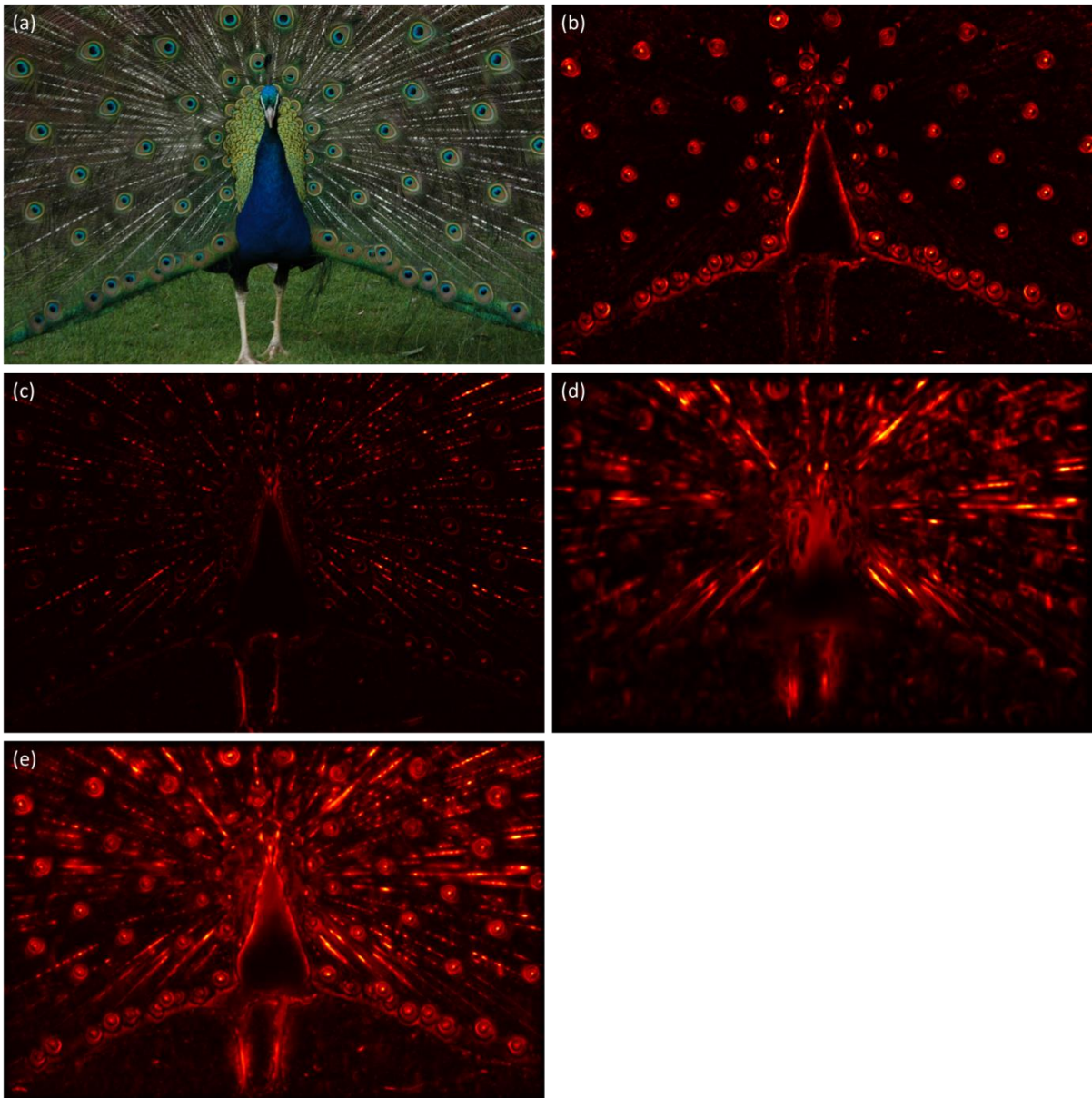
707

708

709

710

711



712

713 Figure 6. (a) Calibrated colour image of a displaying peacock (*Pavo cristatus*), and the  
 714 conspicuity maps for (b) colour, (c) luminance and (d) orientation that result from applying  
 715 the model of visual salience used in this paper. (e) The final overall saliency map. In each  
 716 map, colour is proportional to salience, with lighter colours denoting regions of relatively  
 717 high salience and darker colours regions of relatively low salience. The procedure used was  
 718 as described for experiment 2, but using data on the peafowl's photoreceptor spectral  
 719 sensitivity from Hart (2002).